

Evidence for $O(2)$ universality at the finite temperature transition for lattice QCD with 2 flavours of massless staggered quarks

J. B. Kogut*

Department of Energy, Division of High Energy Physics, Washington, DC 20585, USA

and

Dept. of Physics – TQHN, Univ. of Maryland,

82 Regents Dr., College Park, MD 20742, USA

D. K. Sinclair†

HEP Division, Argonne National Laboratory,

9700 South Cass Avenue, Argonne, IL 60439, USA

Abstract

We simulate lattice QCD with 2 flavours of massless quarks on lattices of temporal extent $N_t = 8$, to study the finite temperature transition from hadronic matter to a quark-gluon plasma. A modified action which incorporates an irrelevant chiral 4-fermion interaction is used, which allows simulations at zero quark mass. We obtain excellent fits of the chiral condensates to the magnetizations of a 3-dimensional $O(2)$ spin model on lattices small enough to model the finite size effects. This gives predictions for correlation lengths and chiral susceptibilities from the corresponding spin-model quantities. These are in good agreement with our measurements over the relevant range of parameters. Binder cumulants are measured, but the errors are too large to draw definite conclusions. From the properties of the $O(2)$ spin model on the relatively small lattices with which we fit our ‘data’, we can see why earlier attempts to fit staggered lattice data to leading-order infinite-volume scaling functions, as well as finite size scaling studies, failed and led to erroneous conclusions.

*Supported in part by NSF grant NSF PHY03-04252.

†This work was supported by the U.S. Department of Energy, Division of High Energy Physics, Contract W-31-109-ENG-38.

I. INTRODUCTION

When hadronic matter is heated to temperatures of 150–200 MeV it makes a transition to a quark-gluon plasma. Such temperatures were present in the early universe. There is also evidence that temperatures this high can be observed in relativistic heavy-ion colliders such as RHIC. Indeed, claims that the quark-gluon plasma has been observed have been made at RHIC and at CERN.

Lattice QCD enables one to simulate QCD at finite temperature and to examine the nature of this transition. When hadronic matter passes through this transition to the quark-gluon plasma, quarks and gluons are no longer confined. In addition, the approximate chiral symmetry associated with light quarks, which is broken spontaneously in cold hadronic matter, is restored. If we reduce the quark mass to zero, this transition must necessarily become a phase transition. We will consider the case of 2 light quarks (u and d), and take their masses to zero, assuming that the strange quark, which we neglect, is too heavy to induce a first-order transition. For 2 light quark flavours, it is believed that the zero-mass transition is a second-order phase transition, which becomes a crossover with no true phase transition as soon as the quarks gain mass [1]. It is argued that the universality class of this phase transition is that of a 3-dimensional $O(4)$ spin model [1]. (Since the symmetry of massless 2-flavour QCD is $SU(2) \times SU(2)$, which is isomorphic to $O(4)$, the π - σ multiplet which provides the Goldstone pions, expresses $O(4)$ symmetry.) The reduced symmetry of staggered quarks reduces this symmetry to $O(2)$, so we might expect that lattice QCD with 2 staggered quark flavours has a phase transition in the universality class of the 3-dimensional $O(2)$ spin model.

In the standard formulations of lattice QCD, the Dirac operator becomes singular at zero quark mass, and so zero-mass simulations are impossible and very light quark simulations become very expensive. We have introduced a modified version of the staggered quark action, which has an additional irrelevant chiral 4-fermion interaction, “ χ QCD” [2]. Being irrelevant, this 4-fermion interaction does not affect the continuum limit, but it does render the Dirac operator non-singular, even in the chiral limit. Hence we simulate 2-flavour QCD with massless quarks using the χ QCD action.

We present the results of simulations of massless two-flavour χ QCD on $N_t = 8$ ($12^3 \times 8$, $16^3 \times 8$ and $24^3 \times 8$) lattices, in the neighbourhood of the finite-temperature transition.

State-of-the-art simulations with conventional and highly improved staggered-quark actions have been run at masses which are too large to accurately determine the universality class of the transition [3, 4]. As a consequence, attempts to determine the universality class of this transition, or to fit its scaling properties under the assumption that they are those for $O(4)$ or $O(2)$ have produced confusing results [5, 6, 7, 8, 9, 10, 11, 12].

Our earlier work on $N_t = 4$ [2, 13] and $N_t = 6$ [14, 15] lattices had produced results which appeared to preclude either $O(2)$ or $O(4)$ universality. We had hoped that running at $N_t = 8$ would broaden the transition sufficiently to allow a better determination of its nature. However, preliminary analysis of our measurements indicated that the chiral condensate decreases too fast for an $O(2)$ or $O(4)$ interpretation. The major problem appears to be that our ‘data’ needs to be extrapolated to infinite volume, and all such extrapolations became unreliable close to the transition. For this reason we abandoned our attempts to extrapolate to infinite volume, and instead fit our chiral condensates to the magnetization curves for the 3-dimensional $O(2)$ spin model, also on finite volumes. By choosing the lattice volumes for best fits, we are able to find good fits to our chiral condensates over most of the range of our measurements. We are also able to use our spin model fits to make acceptable predictions for the correlation lengths and chiral susceptibilities.

Once we establish that the behaviour of lattice QCD appears to be consistent with that of the $O(2)$ spin model, we are able to use the properties of this simple model obtained both from our own simulations and the extensive literature on this model [12, 16, 17, 18, 19, 20] to understand why naive attempts to establish $O(2)$ universality failed. The sizes of the $O(2)$ lattices that give good fits to our χ QCD ‘data’ are too small (5^3 – 9^3) to be anywhere close to the infinite volume limit. In addition, the region over which the leading term suffices to describe the critical scaling of the magnetization of the $O(2)$ spin model in the infinite volume limit is very narrow [16]. A finite size scaling analysis of the $O(2)$ spin model’s magnetization reveals how easy it is to misidentify the universality class of the transition, when only small-lattice data is available.

In section 2 we introduce χ QCD. Section 3 introduces the $O(2)$ spin model and its critical behaviour. We describe our $N_t = 8$ χ QCD simulations and present some of our results in section 4. In section 5 we present our analysis of the χ QCD ‘data’ using the $O(2)$ spin model. Section 6 is devoted to discussions and conclusions.

II. “ χ QCD”

In χ QCD, the lattice Dirac operator is

$$A = \mathcal{D} + m + \frac{1}{16} \sum_i (\sigma_i + i\epsilon\pi_i) \quad (1)$$

where the first 2 terms are the standard staggered quark Dirac operator for quarks in the fundamental representation of colour $SU(3)$, in interaction with the gauge fields on the links of the lattice. The auxiliary fields σ and π are defined on the sites of the dual lattice and the sum is over the 16 sites of the dual lattice closest to the site on which the quark field resides. $\epsilon(x) = (-1)^{x+y+z+t}$. The action for these auxiliary fields is

$$S_{\sigma\pi} = \sum_{\bar{s}} \frac{1}{8} N_f \gamma (\sigma^2 + \pi^2) \quad (2)$$

where the sum is over the sites of the dual lattice. Since this action is completely local, these auxiliary fields can be integrated out introducing a 4-fermion interaction with coupling inversely proportional to γ . χ QCD preserves the remnant $U(1)$ chiral symmetry of the standard staggered quark action for massless quarks. The gauge-field action is the standard Wilson action.

We use hybrid molecular-dynamics simulations to incorporate the factor of $[\det(A^\dagger A)]^{N_f/8}$ in our simulations. Note that, in contrast to the standard staggered Dirac operator, $A^\dagger A$ mixes even and odd lattice sites so that we cannot take the square root of the determinant by restricting our noisy fermion fields to even (or odd) sites.

III. THE $O(2)$ SPIN MODEL IN 3 DIMENSIONS AND CRITICAL BEHAVIOUR

The simplest version of the $O(2)$ spin model in 3 dimensions is a non-linear $O(2)$ sigma model. The Hamiltonian \mathcal{H} (strictly \mathcal{H}/T in condensed matter physics or the action if we are studying this model as a field theory) is given by

$$\mathcal{H} = -J \sum_{\langle i,j \rangle} \mathbf{s}_i \cdot \mathbf{s}_j - \mathbf{H} \cdot \sum_i \mathbf{s}_i, \quad (3)$$

where i and j label sites on a 3 dimensional cubic lattice and $\langle i, j \rangle$ run over all pairs of nearest-neighbour sites. The spins \mathbf{s} are 2-vectors of unit length. \mathbf{H} is an external, symmetry-breaking magnetic field. It is useful to define a temperature T by $T = 1/J$. This

model and variants have been studied extensively in the literature. Papers we have found especially useful are listed in references [12, 16, 17, 18, 19, 20].

The magnetization \mathbf{M} of this system is defined as the lattice average of the spins

$$\mathbf{M} = \frac{1}{V} \sum_i \mathbf{s}_i, \quad (4)$$

where V is the volume of the lattice. We first consider the thermodynamic limit $V \rightarrow \infty$. At $\mathbf{H} = \mathbf{0}$, in the low temperature phase, $O(2)$ is broken by a spontaneous magnetization with its associated Goldstone mode. At high temperatures the magnetization vanishes and $O(2)$ symmetry is restored. The phase transition occurs at a critical point $T = T_c = 1/J_c$ with $J_c = 0.454165(4)$ [19].

Now let us define those critical exponents and amplitudes which describe the critical behaviour of this model and which are relevant to what we might hope to measure. Note that these definitions are more general than this specific model. One defines a reduced temperature t by $t = (T - T_c)/T_c$. We first consider the case $\mathbf{H} = \mathbf{0}$. As $t \rightarrow 0^-$ the magnetization vanishes as

$$M = B(-t)^{\beta_m}. \quad (5)$$

As $t \rightarrow 0^+$, the correlation length

$$\xi = z^+ t^{-\nu}, \quad (6)$$

and the susceptibility

$$\chi = C^+ t^{-\gamma_m}. \quad (7)$$

Here the susceptibility χ is defined by

$$\chi = V \langle M^2 \rangle. \quad (8)$$

The correlation length ξ can be defined in a number of different ways. We will use the second moment formula

$$\xi = \left[\frac{\chi/F - 1}{4 \sin^2(\pi/L)} \right]^{\frac{1}{2}} \quad (9)$$

where L is the length of the box and F is defined by

$$F = \frac{1}{V} \left\langle \left| \sum_i \exp(ip_z z) \mathbf{s}_i \right|^2 \right\rangle \quad (10)$$

where z is the third coordinate of the site \mathbf{i} and $p_z = 2\pi/L$. This form for ξ appears to have originated with reference [21]. At small but non-zero H , the magnetization

$$M = dH^{\frac{1}{\delta}}. \quad (11)$$

For the $O(2)$ spin model these critical exponents have (approximate) values $\beta_m = 0.3490(6)$, $\nu = 0.6723(11)$, $\gamma_m \approx 1.32$, $\delta \approx 4.7798$, $\omega = 0.79(2)$ (ω is a critical exponent parameterizing finite size corrections).

More information can be obtained about critical points by measuring fluctuation quantities (in addition to the susceptibility). One such quantity is the fourth-order Binder cumulant

$$B_4 = \frac{\langle M^4 \rangle}{\langle M^2 \rangle^2}. \quad (12)$$

For $H = 0$ on an infinite lattice, this quantity is 1, the value for a first-order transition, for $T < T_c$, and 2, the value for a crossover, for $T > T_c$. Right at T_c it has been measured at $B_4 = 1.242(2)$ for the $O(2)$ spin model [17]. On a finite lattice there is a smooth crossover from 1 to 2 as T is varied from small to large values, crossing T_c . This crossover steepens as V is increased. For large V s a finite size scaling analysis indicates that these curves cross at points which approach $[T_c, B_4(T_c)]$ as $V \rightarrow \infty$. Similarly curves of ξ/L for finite L (and hence V) cross at points which approach T_c and a universal value $[\xi/L](T_c) = 0.593(2)$, a value specific to $O(2)$.

Working at finite volume, where $\langle \mathbf{M} \rangle = \mathbf{0}$, it is necessary to find an alternative definition of the ensemble-averaged magnetization. One which has proved useful is

$$M = \langle |\mathbf{M}| \rangle, \quad (13)$$

which will approach the value of the spontaneous magnetization as $V \rightarrow \infty$. It is clear, however, that this quantity does not vanish in the high temperature phase except in the infinite volume limit. Hence, to test that it has the correct critical behaviour or to measure the critical exponent β_m , it is necessary either to extrapolate to infinite volume, or to apply a finite size scaling analysis. Finite size scaling for M predicts that close to the critical point [22]

$$M(t, L) = L^{-\frac{\beta_m}{\nu}} [Q(tL^{\frac{1}{\nu}}) + L^{-\omega} G(tL^{\frac{1}{\nu}}) + \dots] \quad (14)$$

so that plotting $L^{\frac{\beta_m}{\nu}} M$ against $tL^{\frac{1}{\nu}}$ should make the magnetization curves for different L values coincide, provided L is sufficiently large.

For QCD, the chiral condensate plays the rôle of the magnetization. In the 2-dimensional space of the remnant $U(1)$ or $O(2)$ symmetry of staggered fermions, the chiral condensate $(\bar{\psi}\psi, i\bar{\psi}\gamma_5\xi_5\psi)$ or (σ, π) corresponds to the magnetization of the $O(2)$ spin model.

IV. χ QCD SIMULATIONS ON $N_t = 8$ LATTICES

We have performed high statistics simulations of massless 2-flavour χ QCD on $16^3 \times 8$ and $24^3 \times 8$ lattices and lower statistics simulations on $12^3 \times 8$ lattices, using the hybrid molecular-dynamics algorithm with $dt = 0.05$. Measurements are made every 2 1-time-unit trajectories. For these simulations the parameter γ was fixed at 10. At each of 6 values of $\beta = 6/g^2$ close to the transition ($\beta = 5.5250, 5.5275, 5.5300, 5.5325, 5.5350, 5.5375$) we ran for 100,000 trajectories on each of the two larger lattices. For $\beta = 5.5400, 5.5450, 5.5500$ we ran for 50,000 trajectories on each of the 2 larger lattices. Shorter runs were made for β values outside of this range.

Figure 1 shows the chiral condensate and Wilson line (Polyakov loop) as functions of $\beta = 6/g^2$ for both the $16^3 \times 8$ and the $24^3 \times 8$ lattices. From this figure, it is clear that the finite temperature phase transition occurs somewhere in the range $5.53 \lesssim \beta \lesssim 5.54$. The smoothness of the transition suggests strongly that it is second order. The curvature of the chiral condensate for the larger lattice (before finite volume rounding sets in) indicates that $\beta_m < 1$, something that the best finite mass simulations to date have difficulty in observing. The reason that such high statistics are needed becomes clearer when one looks at the time histories of observables measured during these runs. In figure 2 we show the time history of the chiral condensate on the $24^3 \times 8$ lattice for $\beta = 5.535$ which is close to the transition, and $\beta = 5.5325$ which is just below the transition. Because of critical slowing down, the system shows fluctuations which last for thousands of trajectories close to the critical point.

With the standard staggered action at zero quark mass, the chiral condensate vanishes identically on each configuration, so even if we could simulate at $m = 0$ we could not observe a chiral condensate, even on a configuration by configuration basis. This has to be true because the remnant $U(1)$ chiral symmetry is manifest at any fixed value of the gauge fields, i.e. on each configuration, which precludes the existence of a chiral condensate. With the χ QCD action, the condensate is finite on each configuration. This is because, a configuration consists of a set of gauge fields *and* a set of auxiliary fields σ and π . Any non-

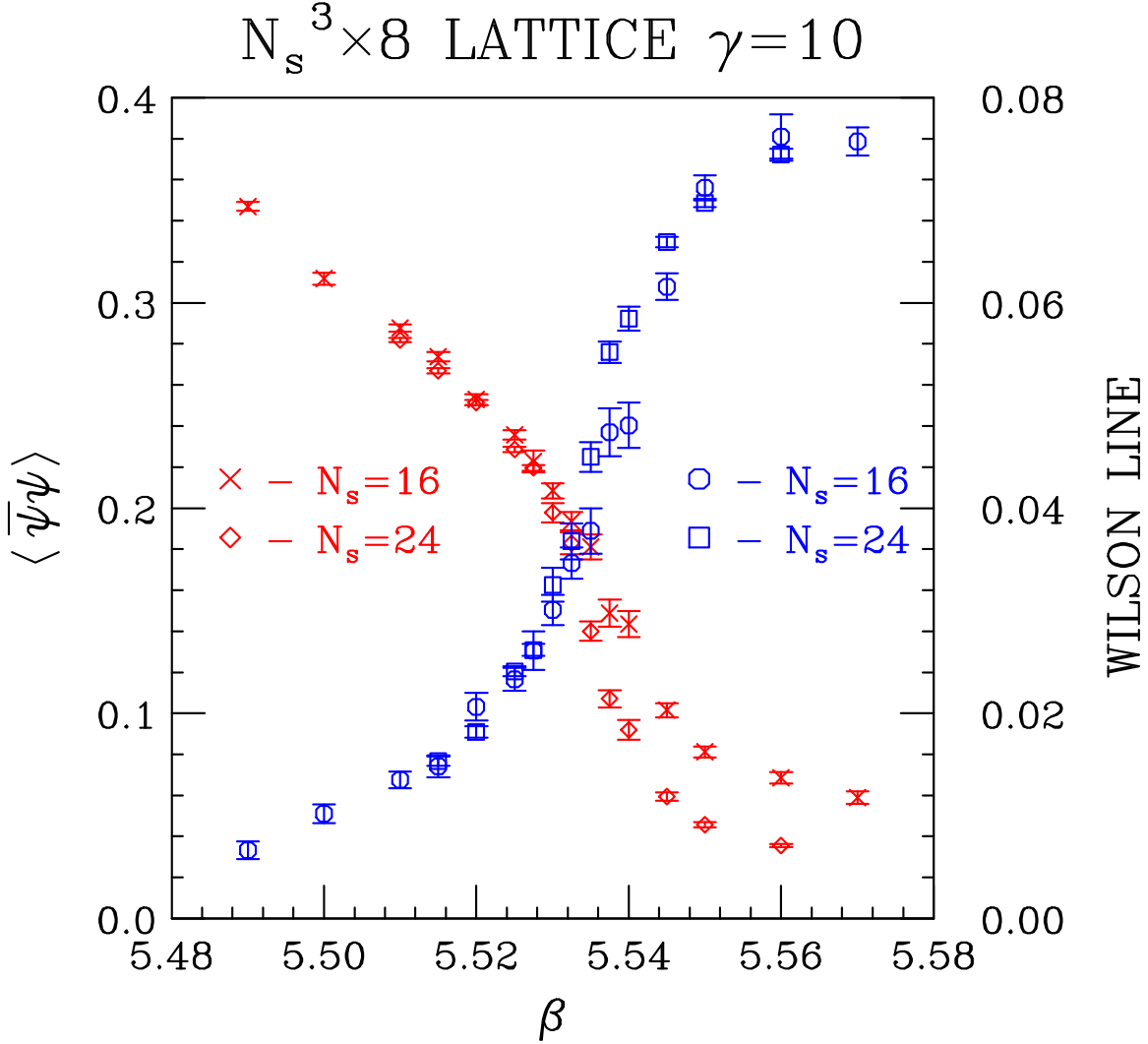


FIG. 1: Chiral condensate and Wilson Line as functions of $\beta = 6/g^2$ for $16^3 \times 8$ and $24^3 \times 8$ lattices.

zero set of auxiliary fields breaks chiral symmetry. The vanishing of the chiral condensate on a finite volume occurs because, as the system evolves in molecular-dynamics ‘time’, the condensate rotates in the $(\bar{\psi}\psi, i\bar{\psi}\gamma_5\xi_5\psi)$ plane so that the ensemble average is zero. This is because all $U(1)$ global chiral rotations of the auxiliary fields contribute to the ensemble of configurations with equal weight. What we have called $\langle \bar{\psi}\psi \rangle$ in the figures above is really $\langle \sqrt{\bar{\psi}\psi^2 - \bar{\psi}\gamma_5\xi_5\psi^2} \rangle$ where the quantities under the square root are lattice averaged before being squared. Similarly we define a quantity which we denote $\langle \sigma \rangle$ which is really $\langle \sqrt{\sigma^2 + \pi^2} \rangle$. In the infinite volume limit each of these quantities will approach the condensate of interest. These condensates are related by

$$\langle \bar{\psi}\psi \rangle = \gamma \langle \sigma \rangle \quad (15)$$

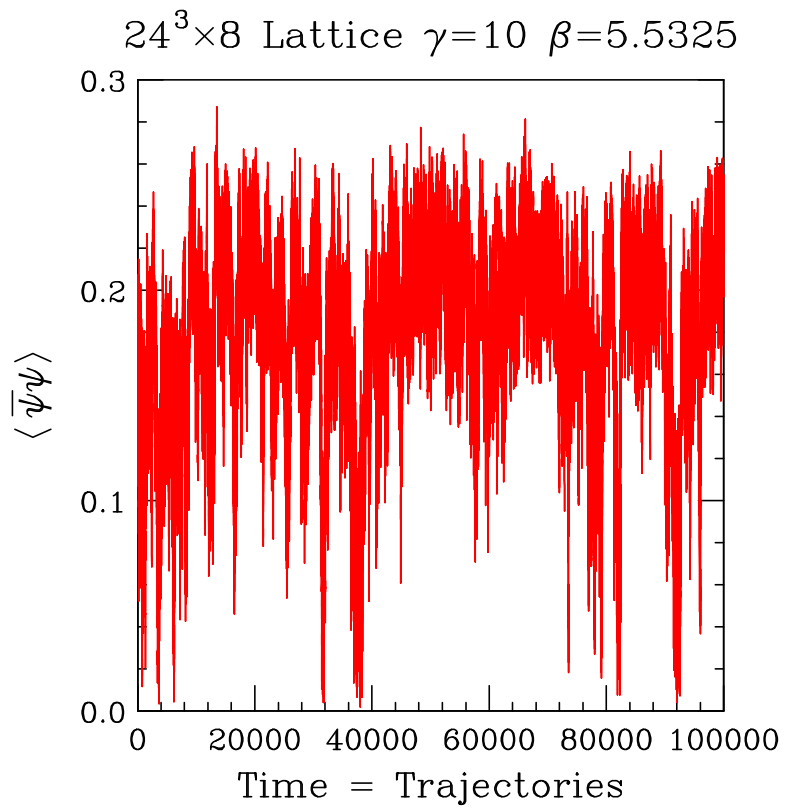
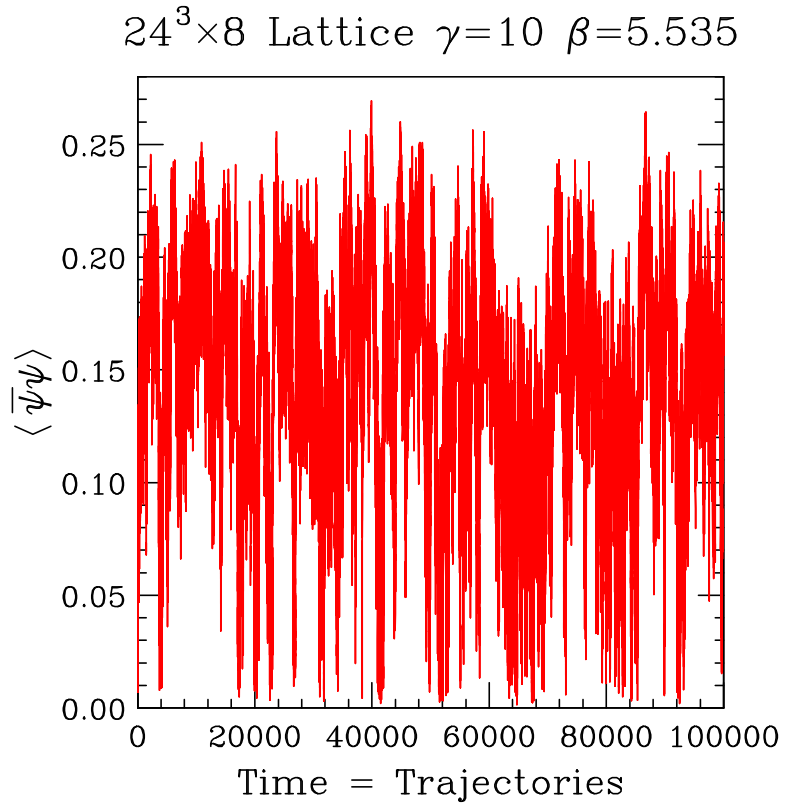


FIG. 2: Time histories of the chiral condensate on a $24^3 \times 8$ lattice a) for $\beta = 5.535$ b) for $\beta = 5.5325$.

at $dt = 0$, (at least in the infinite volume limit) so either quantity can be used as the chiral condensate. This will be important when we consider fluctuation quantities, since the ‘ $\bar{\psi}\psi$ ’ we measure is only a stochastic estimator of the condensate, while σ is a true condensate. Figure 3 is a scatter-plot of the actual chiral condensates measured in the $(\bar{\psi}\psi, i\bar{\psi}\gamma_5\xi_5\psi)$ plane on individual configurations for 3 β values close to the transition, on a $24^3 \times 8$ lattice. One should first note that the condensate does indeed rotate in the plane between configurations so that the ensemble average is zero, even in the ordered phase. At $\beta = 5.5325$, below the transition, the distribution is concentrated in a ring, indicating a non-zero condensate. By $\beta = 5.5350$, close to the transition, the ring structure is no longer clear, although a peak away from the origin still shows up on a radial density profile. Finally, for $\beta = 5.5375$, above the transition, the maximum density is at the origin indicating that the condensate has vanished, and chiral symmetry is restored.

In the figure 1 it is clear that to attempt fits to the leading critical scaling behaviour

$$\langle\bar{\psi}\psi\rangle = b(\beta_c - \beta)^{\beta_m} \quad \beta < \beta_c, \quad (16)$$

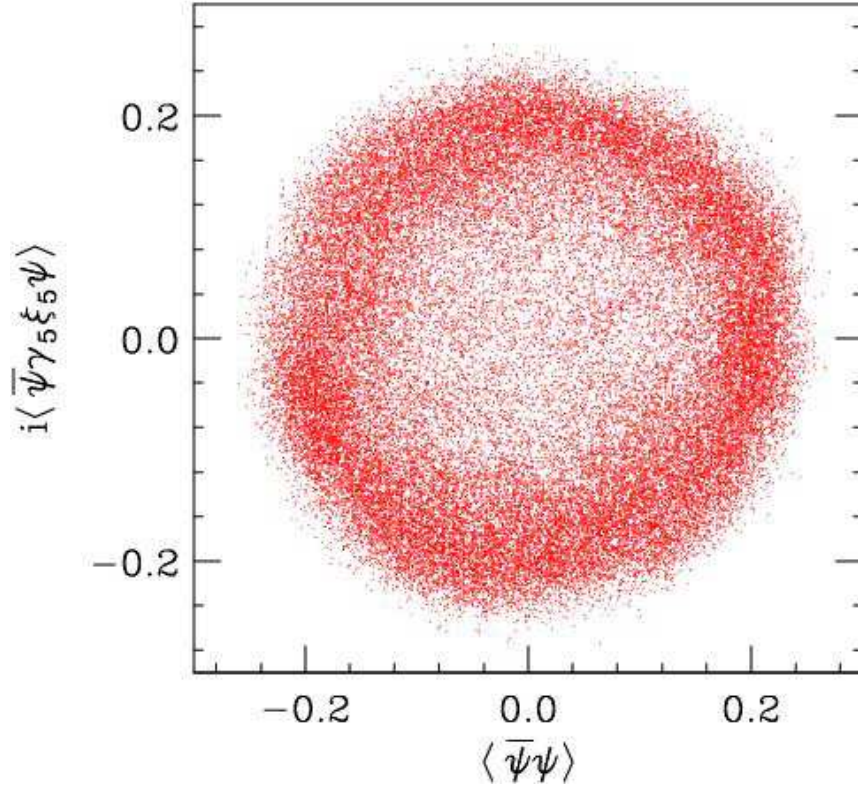
requires continuation to infinite volume. Unfortunately, such extrapolations break down close to the transition, which is where accurate measurements are most needed. Fits to any of these attempted extrapolations always favour values of β_m much smaller than that of the 3-dimensional $O(2)$ spin model. It is for this reason that we have tried fitting to the magnetization curves for the $O(2)$ spin model on *small* lattices which also incorporate finite volume effects.

Binder cumulants [23] have been found useful in characterizing phase transitions. Figure 4 shows the 4th order Binder cumulants for the auxiliary fields (σ, π) . Following the definitions given in the previous section, B_4 is defined by

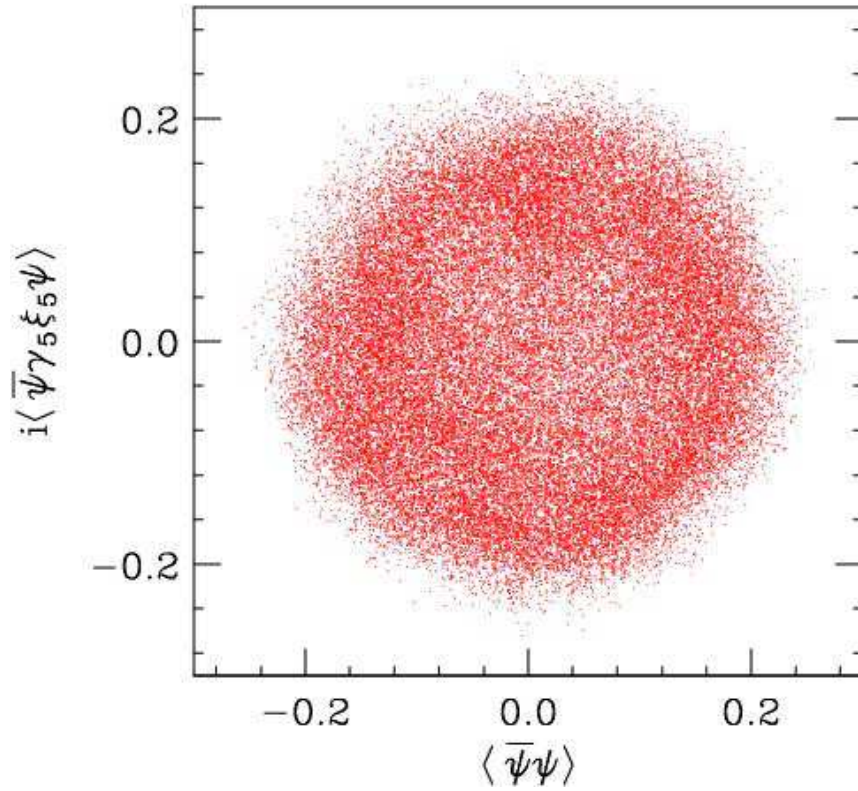
$$B_4 = \frac{\langle(\sigma^2 + \pi^2)^2\rangle}{\langle\sigma^2 + \pi^2\rangle^2} \quad (17)$$

For low β , B_4 does appear to approach 1 as expected for a first order transition (this is the first order transition when the mass m passes through zero, causing the condensate to abruptly change sign). At high β , B_4 does appear to approach 2, the value for a crossover, as expected. In between the curves for the 3 lattice sizes do appear to cross at an intermediate value, which is characteristic of a second order transition. The statistics are not good enough to determine the positions or values of these intersections, but they appear to be higher than

$24^3 \times 8$ LATTICE $\beta=5.5325$ $\gamma=10$ $m=0$



$24^3 \times 8$ LATTICE $\beta=5.535$ $\gamma=10$ $m=0$



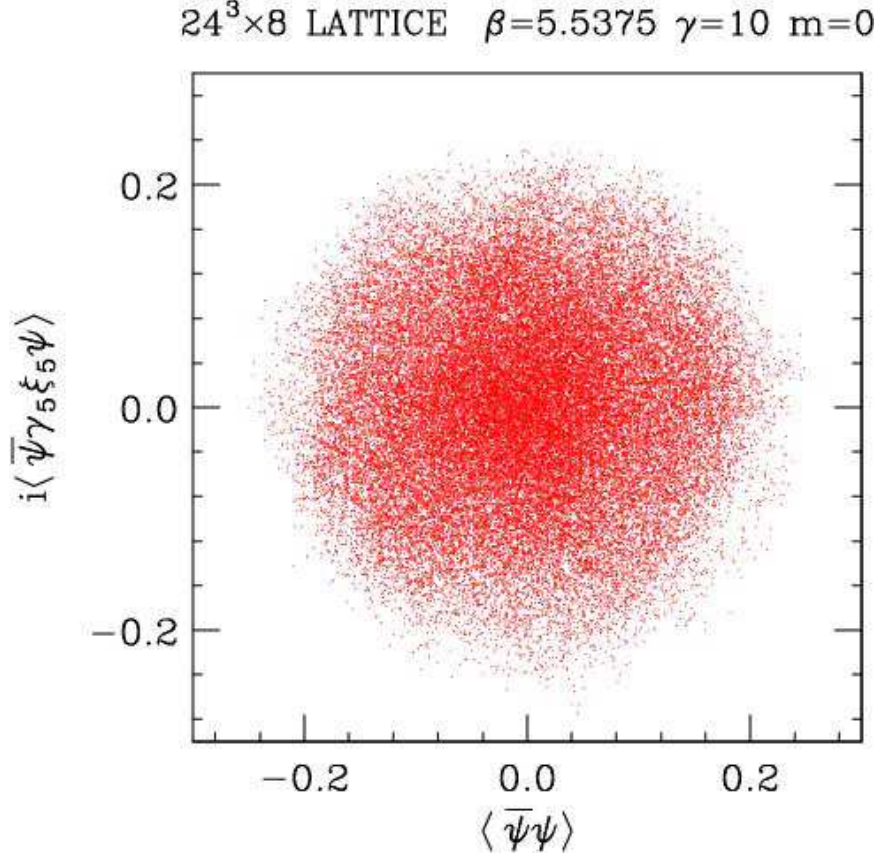


FIG. 3: Scatter-plots of the chiral condensates on a $24^3 \times 8$ lattice. Each of the 50,000 points on each graph represents the value on a single configuration the angle brackets here indicate that these are configuration averaged quantities but *not* ensemble averages. a) $\beta = 5.5325$, b) $\beta = 5.5350$, c) $\beta = 5.5375$.

the value 1.242(2) expected if the transition were in the $O(2)$ universality class. However, this probably indicates that our lattices are too small for this intersection to occur very close to the infinite volume value. However, this powerful technique should be an excellent way of determining the nature of the transitions for larger lattices with very high statistics.

To get estimates of the position of the transition directly from the ‘data’ (rather than from the fits to spin-model curves) we look at the radial chiral susceptibility, expressed in terms of the auxiliary fields

$$\chi_r(\boldsymbol{\sigma}) = V(\langle |\boldsymbol{\sigma}|^2 \rangle - \langle |\boldsymbol{\sigma}| \rangle^2), \quad (18)$$

where $\boldsymbol{\sigma} = (\sigma, \pi)$. The position of the phase transition is estimated from the peak of this susceptibility, which is found using Ferrenberg-Swendsen reweighting [24] to interpolate our

$N_s^3 \times 8$ LATTICE $\gamma=10$

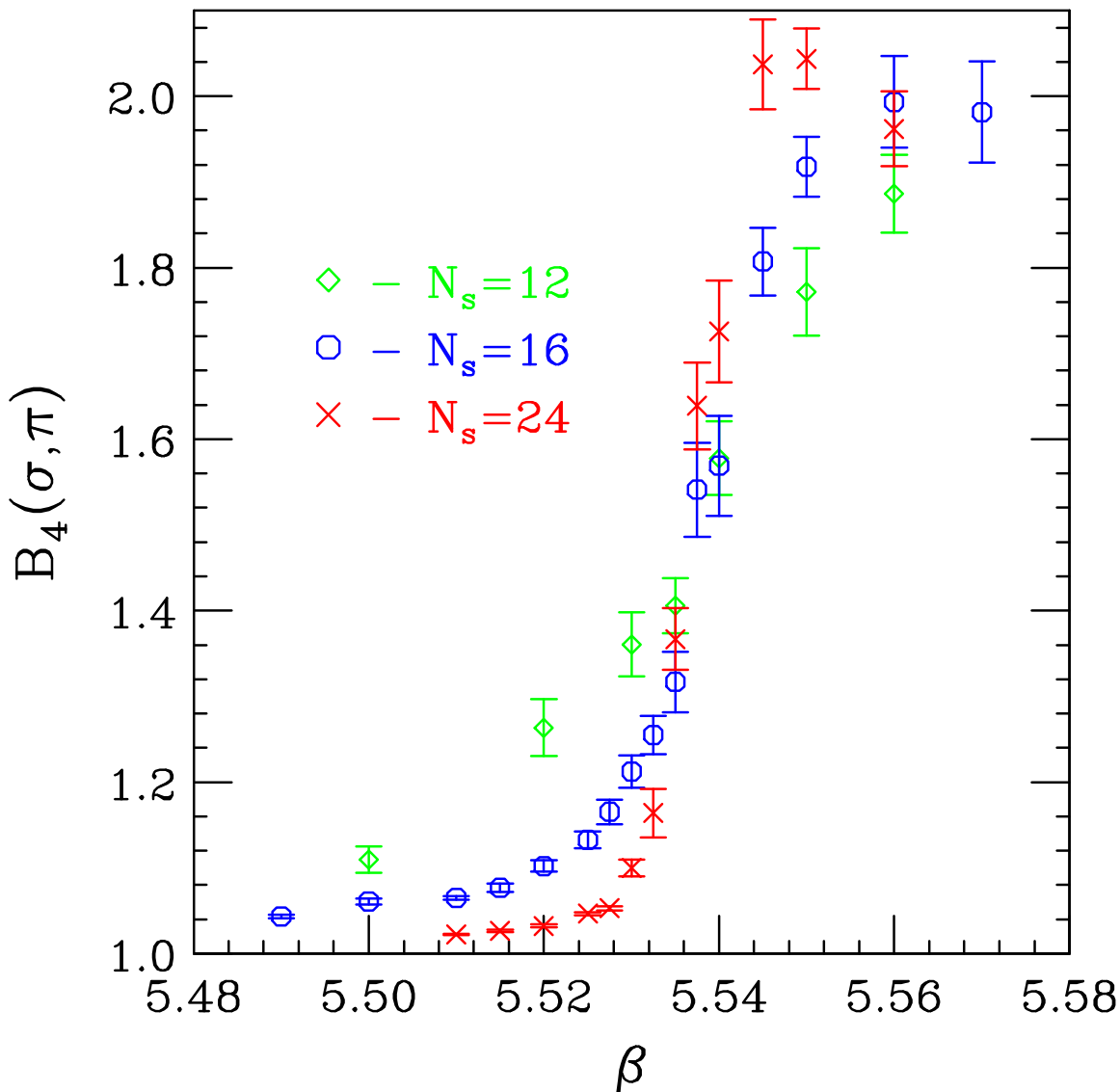


FIG. 4: The fourth-order binder cumulants for the auxiliary fields as functions of β for $12^3 \times 8$, $16^3 \times 8$ and $24^3 \times 8$ lattices.

‘data’. This yields an estimate of $\beta_c = 5.5390(6)$ for the $16^3 \times 8$ lattice and $\beta_c = 5.5359(5)$ for the $24^3 \times 8$ lattice. (Note that we have also tried using Ferrenberg-Swendsen reweighting to interpolate the ‘data’ for our condensates. While this indicates that the interpolations from the measurements at β values at the ends of each interval are consistent, the curves it yields at current statistics are not sufficiently smooth to help with fits, taking into account that the extra points yielded by these interpolations are highly correlated.) In the next

section we indicate how β_c calculated in this way approaches the infinite volume limit.

V. $O(2)$ SPIN-MODEL ANALYSIS OF χ QCD MEASUREMENTS

We have simulated the 3-dimensional $O(2)$ spin model with the Hamiltonian given in equation 3 on small lattices – 4^3 , 5^3 , 6^3 , 8^3 , 9^3 , 12^3 , 16^3 and 24^3 . These are adequate for the comparisons we make with our results from lattice QCD simulations using the χ QCD action, which were presented in the previous section. For spin-model results on lattices large enough to make comparison with the infinite volume limit, we appeal to the literature. For our 4^3 to 12^3 lattices, we have interpolated our measurements of the magnetization over the range $0 \leq J \leq 1.5$ using Ferrenberg-Swendsen reweighting. Figure 5 shows the results of our $O(2)$ simulations and the scaling curves they produced.

Attempts to perform a finite size scaling analysis (equation 14) around the chiral phase transition of χ QCD with $O(2)$ critical indices fail to indicate the existence of a universal scaling function. Thus, if the critical point of this theory is in the $O(2)$ universality class, finite volume effects on lattices of the size we use are too large to allow the ‘data’ to be fit by a single scaling function.

An alternative approach, is to fit the chiral condensates to the magnetization curves for the $O(2)$ spin models on lattices sufficiently small that they too show finite size departures from the universal scaling function. Note that these departures depend on the specific form of the $O(2)$ spin-model Hamiltonian used (equation 3). We allow ourselves the freedom to vary the spin-model lattice sizes to obtain the best fits to the χ QCD ‘data’. This is justified if a single operator is adequate to describe most of the departures from the $L \rightarrow \infty$ universal scaling function of equation 14 for the $O(2)$ spin model, and the corresponding operator describes most of these departures for χ QCD. Varying the lattice size for the $O(2)$ spin model allows us to match the coefficients of the universal scaling function (presumably the coefficient G of $L^{-\omega}$ in equation 14) which describes this departure. If more than one non-leading term is required for the model of equation 3, modeling non-leading behaviour of χ QCD in this way is somewhat serendipitous. We fit our chiral condensates to the 3-parameter form

$$\langle \bar{\psi}\psi(\beta) \rangle = b \langle M(a(\beta - \beta_c) + T_c) \rangle \quad (19)$$

where $\langle \bar{\psi}\psi \rangle$ is the average of the magnitude of the chiral condensate for χ QCD and $\langle M \rangle$

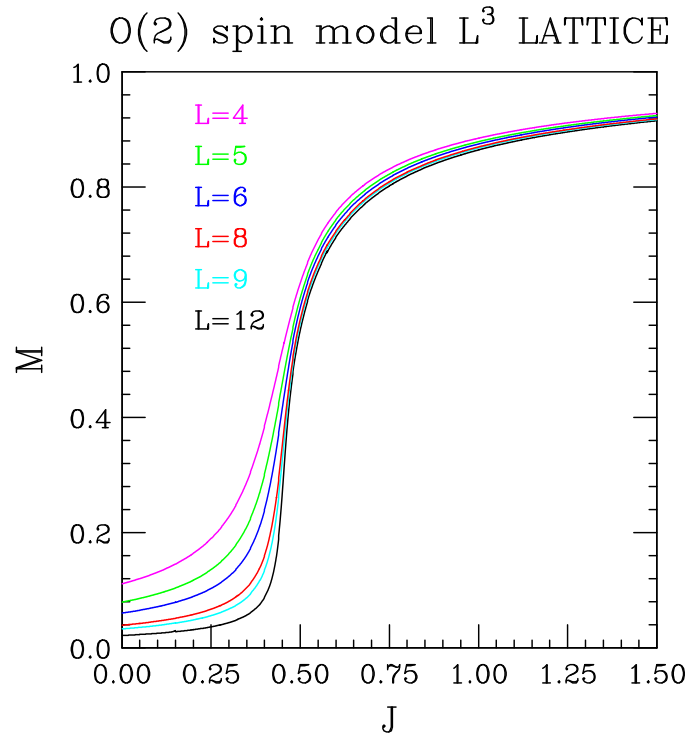
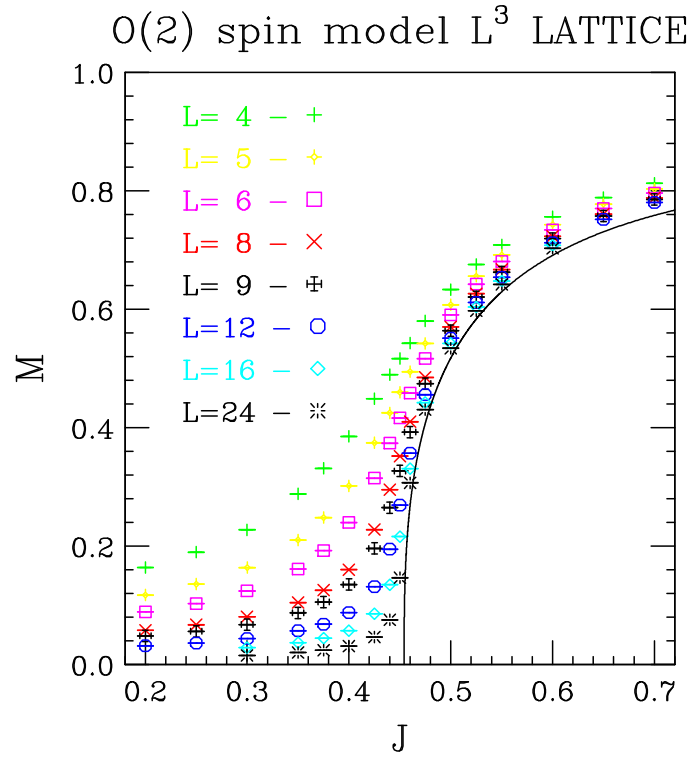


FIG. 5: a) Magnetization as a function of coupling J for the 3-dimensional O(2) spin-model. The curve is a parametrization of the infinite volume limit given in reference [16]. b) Magnetization curves from Ferrenberg-Swendsen reweighting.

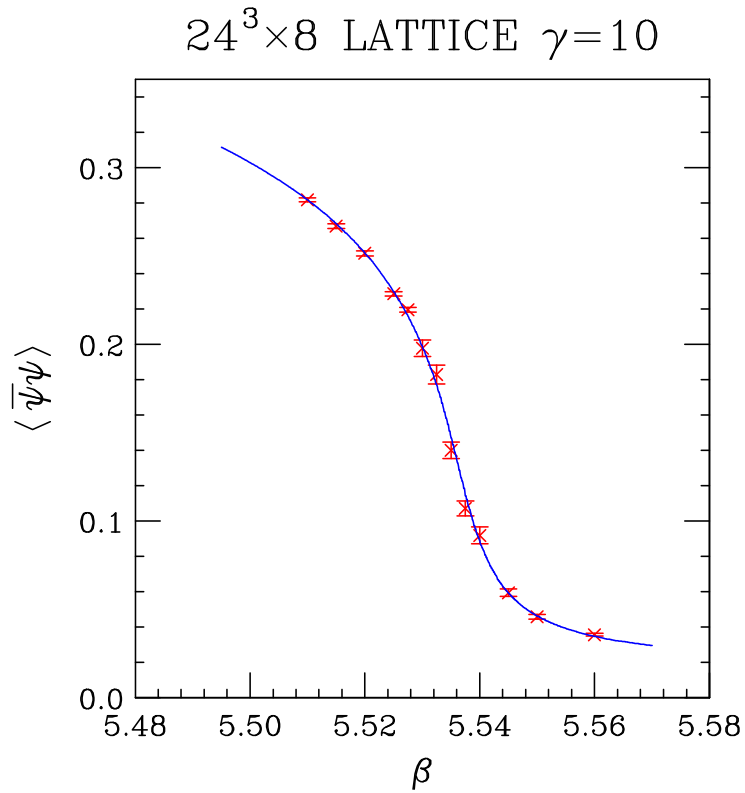
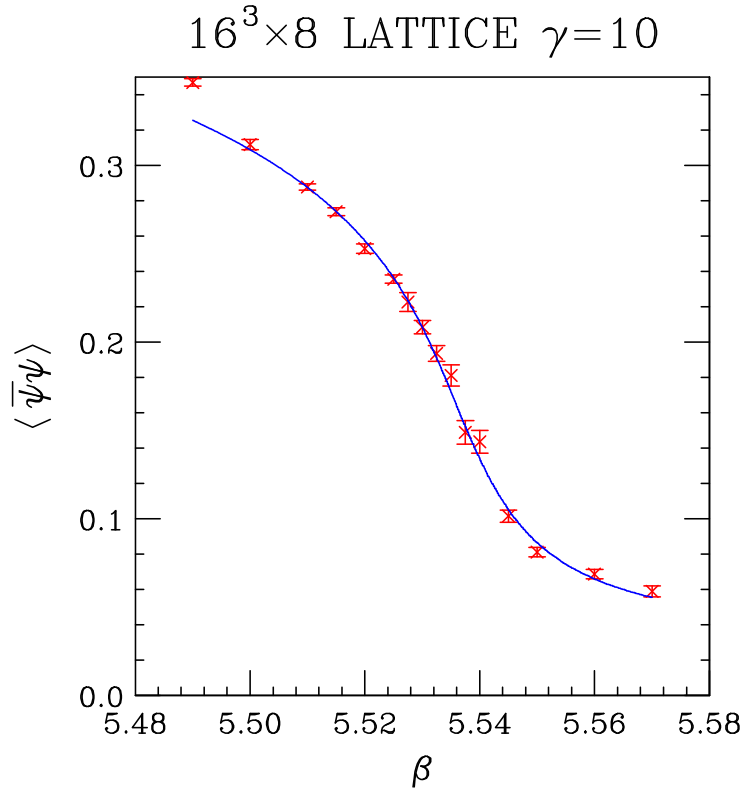


FIG. 6: a) Fit of the chiral condensate for χ QCD on a $16^3 \times 8$ lattice to the magnetization of an $O(2)$ spin model on a 6^3 lattice. b) Fit of the chiral condensate for χ QCD on a $24^3 \times 8$ lattice to the magnetization of an $O(2)$ spin model on an 8^3 lattice.

is the magnetization of the $O(2)$ spin model as a function of $T = 1/J$. $T_c = 1/0.454165$ is taken as the critical temperature of the $O(2)$ spin model. β_c the critical value of $\beta = 6/g^2$; a and b are the parameters of the fit. For the $16^3 \times 8$ lattice condensate, the best fit is to the magnetization on a 6^3 lattice which had a $\chi^2/DOF = 1.36$ with parameters $\beta_c = 5.5358(4)$, $a = 23.7(8)$ and $b = 0.380(4)$ over the range $5.50 \leq \beta \leq 5.57$. Fits to other lattice sizes have $\chi^2/DOF = 2.34$ (4^3), $\chi^2/DOF = 1.58$ (5^3), $\chi^2/DOF = 1.55$ (8^3). For the $24^3 \times 8$ lattice, the best fits to the condensate are to the magnetizations on lattice sizes 6^3 which has $\chi^2/DOF = 1.85$ and parameters $\beta_c = 5.5355(2)$, $a = 53.5(1.3)$, $b = 0.312(2)$ and 8^3 which has $\chi^2/DOF = 1.87$ with $\beta_c = 5.5360(2)$, $a = 30.7(6)$, $b = 0.355(2)$ over the range $5.51 \leq \beta \leq 5.56$. Fits to other lattice sizes have $\chi^2/DOF = 2.63$ (9^3) and $\chi^2/DOF = 3.16$ (5^3). We are able to obtain reasonable fits over a range of lattice sizes, since if our lattice QCD lattices were large enough to be fit by the single scaling function of equation 14, we should be able to obtain good fits of the above form for any $O(2)$ spin-model lattice large enough to also be fit by a single finite-size-scaling function. Figure 6 shows the condensates on $16^3 \times 8$ and $24^3 \times 8$ lattices. The curves are the fits to the $O(2)$ spin models. We have also reanalyzed our ‘data’ from earlier simulations on an $18^3 \times 6$ lattice which we had previously interpreted as showing tricritical scaling. We find that we can fit these measurements to the magnetization for the $O(2)$ spin model on an 8^3 lattice with $\chi^2/DOF = 1.57$. Thus $N_t = 6$ χ QCD also shows consistency with $O(2)$ universality. These fits show the first evidence that the chiral condensates are consistent with $O(2)$ scaling.

We next examine the correlation length ξ , defined as in equation 9 but with σ replacing \mathbf{M} . One observation that has been made in $O(2)$ spin models is that curves for ξ/L (L is the box size) on different (large) lattice sizes cross at a point where $\xi/L = 0.593(2)$ [17], a value which is expected to depend only on the universality class. Figure 7 shows ξ for the 3 lattice sizes of our simulations. This gives some indication that the intersection point of the correlation lengths is rising towards the universal $O(2)$ value as the lattice size is increased. ξ/N_3 for lattice QCD and ξ/L for the spin model should define the same universal scaling function in the high temperature phase (which is the only regime where the definition of equation 9 has the interpretation as a correlation length), at corresponding values of β and T , defined through

$$\beta = (T - T_c)/a + \beta_c, \quad (20)$$

where β_c and a are obtained from the fits of equation 19, except for $\langle \sigma \rangle$ rather than $\langle \bar{\psi}\psi \rangle$.

$N_s^3 \times 8$ LATTICE $\gamma=10$

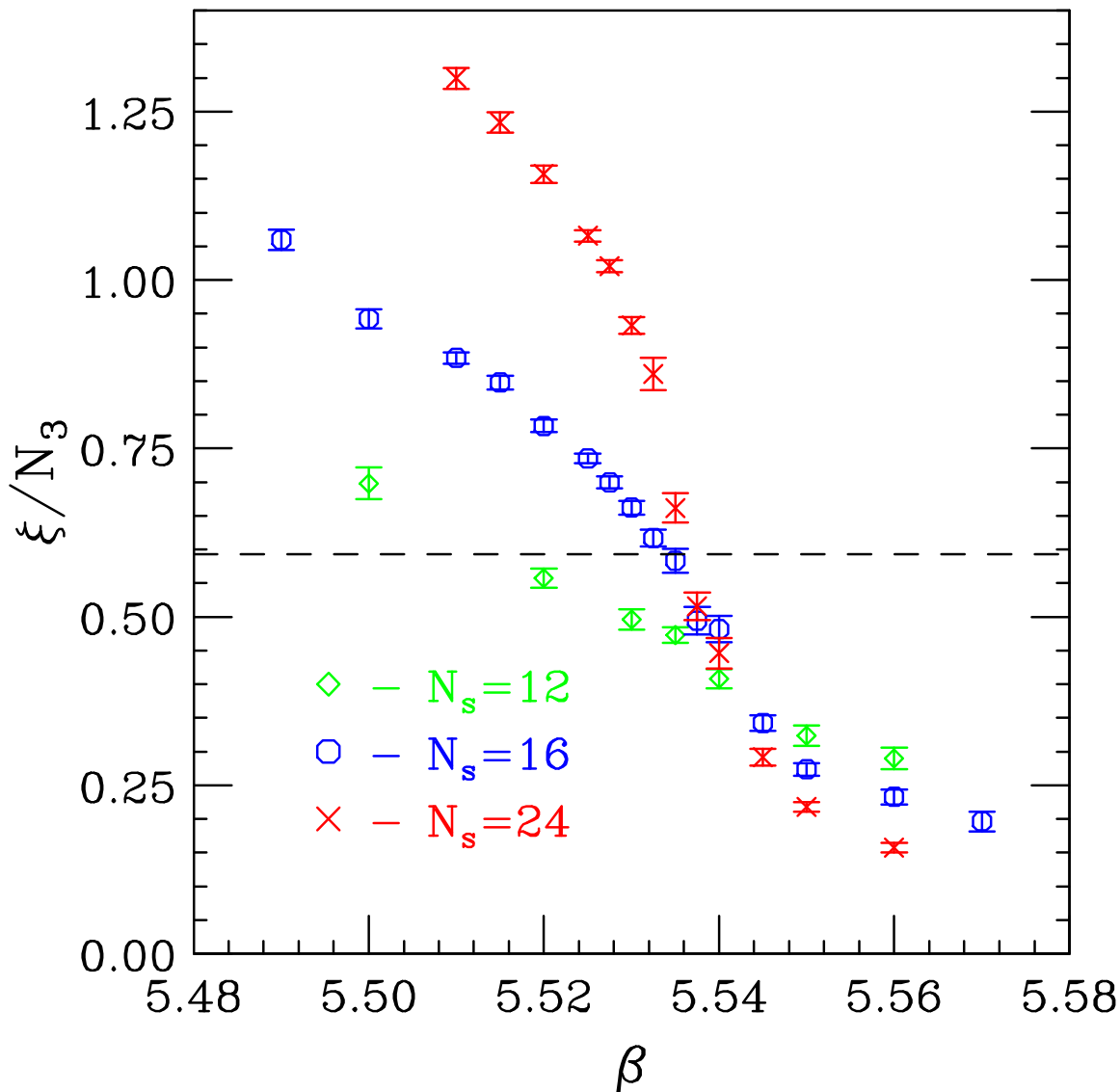


FIG. 7: The second moment correlation lengths ξ as functions of β on $12^3 \times 8$, $16^3 \times 8$ and $24^3 \times 8$ lattices. Note that $N_3 = N_s$ since the spatial ‘box’ is a cube in each case.

In figure 8 we have plotted the values of ξ/N_3 from our χ QCD simulations along with ξ/L from the $O(2)$ lattice sizes which show the best agreement. The agreement for the larger lattice is quite good in the high temperature phase, that for the smaller lattice is only fair.

The final quantity which we wish to compare with the $O(2)$ spin model is the chiral susceptibility, which is the equivalent of that defined in equation 8 with \mathbf{M} replaced by $\boldsymbol{\sigma}$. As with the correlation length discussed above, this really only has the interpretation of

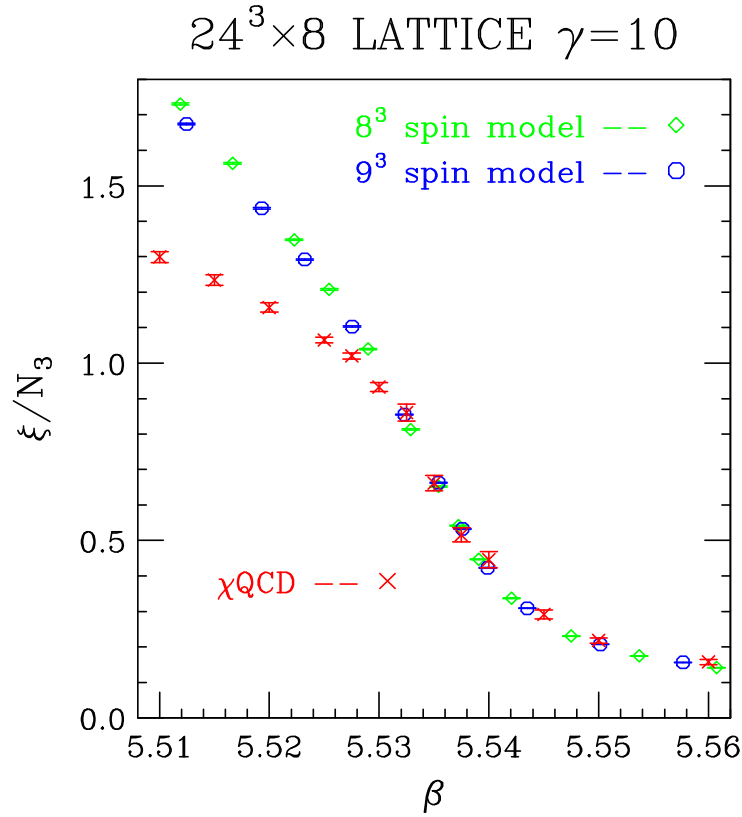
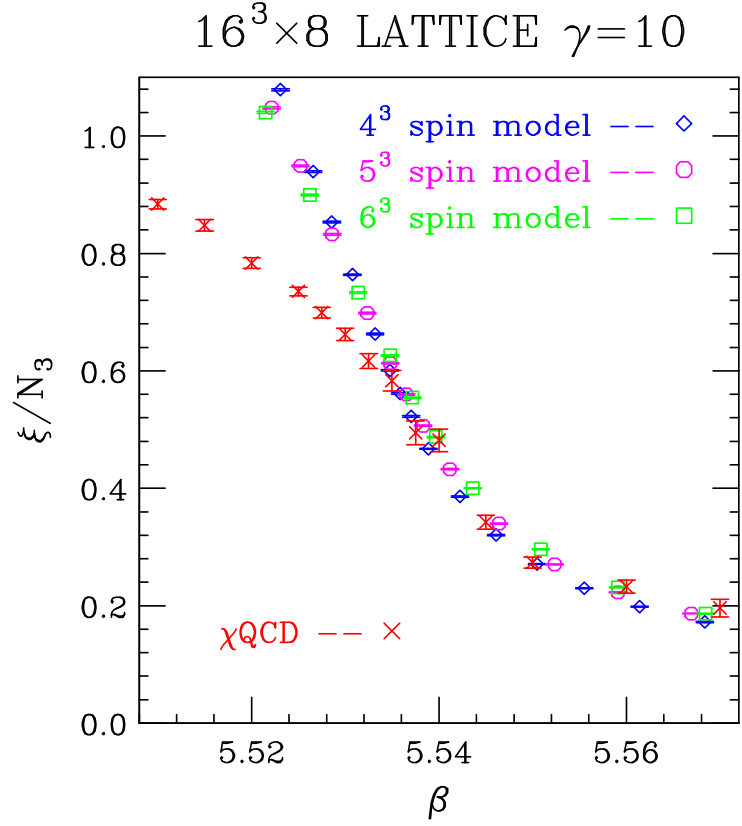


FIG. 8: ξ/N_3 for χ QCD and ξ/L for the $O(2)$ spin model at corresponding beta values: a) for the $16^3 \times 8$ lattice; b) for the $24^3 \times 8$ lattice.

susceptibility in the high temperature domain. The values of a and b from fits of $\langle\sigma\rangle$ using equation 19 give predictions for the chiral susceptibility from the equivalent quantity for the spin model

$$\chi_\sigma = V\langle\sigma^2 + \pi^2\rangle = Vb^2\langle\mathbf{M}^2\rangle. \quad (21)$$

We have plotted these predictions against our χ QCD measurements in figure 9. The agreement between the QCD ‘data’ and spin-model predictions is very good for the $24^3 \times 8$ lattice, less so for the $16^3 \times 8$ lattice.

We have used Ferrenberg-Swendsen reweighting to obtain the peaks of the radial susceptibility for the $O(2)$ spin model as a function of lattice size, from 4^3 to 32^3 lattices. We assume that the position of the peaks scales as

$$J_{peak} = J_c - K L^{-\theta}. \quad (22)$$

This fit yields $J_c = 0.45403(6)$ from a fit from lattice sizes from 6^3 to 32^3 compared with the best estimate from the literature of $J_c = 0.454165(4)$. The same fit yields $\theta = 1.70(2)$ and $K = 0.38(2)$. Hence we conclude that this is a good method for estimating J_c for the spin-model and hence should be reasonable for estimating β_c for χ QCD.

We can now study the $O(2)$ spin model measurements to understand why it is nearly impossible to interpret the critical behaviour of our lattice QCD results directly without comparing them with the spin-model behaviour on small lattices. In reference [16] it was noted that it is only possible to fit the magnetization curve in the infinite volume limit to the leading order critical scaling form of equation 5 over a very small range of $|T_c - T|$ – roughly 0–0.07. In terms of J this means from J_c up to perhaps 0.47. Above J_c , the leading finite-size corrections to the magnetization are of order $1/L$. However, even when J is as large as 0.475 extrapolating in $1/L$ only works for $L \gtrsim 12$. Hence, for the 5^3 to 9^3 lattices which fit our χ QCD ‘data’, we cannot perform the infinite volume extrapolation reliably. In the disordered phase, the leading finite volume corrections are of order $1/\sqrt{V} = 1/L^{3/2}$. [This is true provided $L \gg \xi$, since then one can divide the lattice into $N \propto V$ domains of extent $> \xi$. The orientations of the spins in these domains will be independent of one another so that the magnetization of each spin configuration will be $\mathcal{O}(\sqrt{N}/V)$ i.e. $\mathcal{O}(1/\sqrt{V})$.] By the time J is as large as 0.425, departures from this leading order extrapolation are already visible on the 9^3 lattice. Hence simulations in the region of leading order scaling are inaccessible to the small lattices of interest. Even if they were accessible, they represent

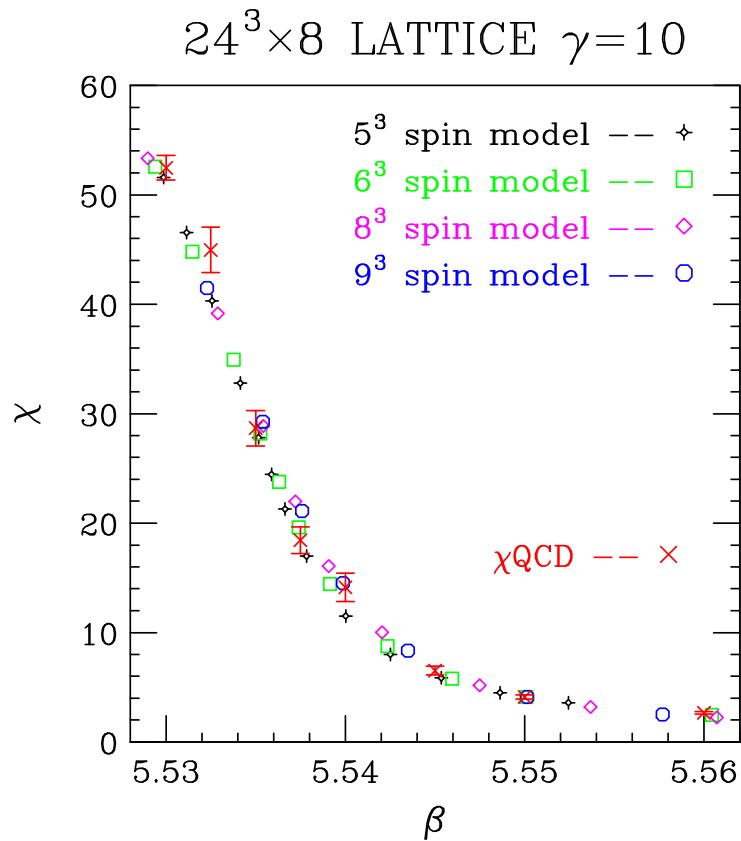
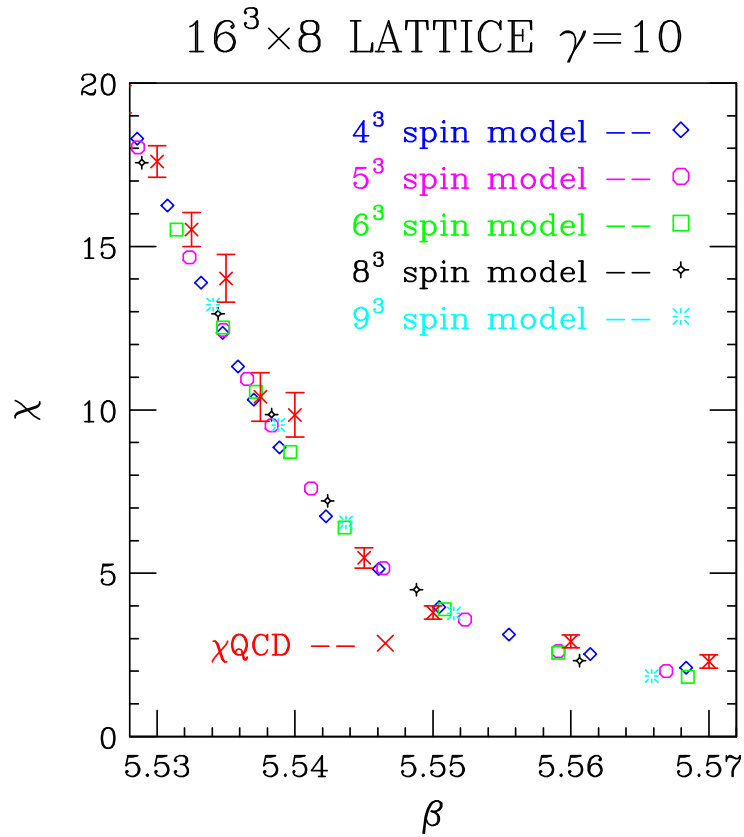


FIG. 9: χ_σ for χ_{QCD} compared with the predictions from χ for the $O(2)$ spin model.

such a small region of β (within ≈ 0.0024 of the transition for the $24^3 \times 8$ lattice) as to contain only 1 or 2 data points. Reference [16] finds good fits to the magnetization over a much larger range using the scaling form

$$M = B(T_c - T)^{\beta_m} [1 + b_1(T_c - T)^{\omega\nu} + b_2(T_c - T)] \quad (23)$$

– this is the curve plotted in figure 5. Even if we fixed all 3 critical exponents to their $O(2)$ values, this still has 4 parameters. By the time we excluded enough points close to the transition and performed the infinite volume extrapolations, such a fit for χ QCD would have little predictive power. As the authors of this paper and reference [18] note, the narrowness of the scaling region appears to be a property peculiar to the $O(2)$ spin model (at least to this particular $O(2)$ spin model). [Note that the leading departure from scaling (the term proportional to b_1) in this form corresponds to that in the finite-size scaling form of equation 14 with $G(x) \rightarrow Bb_1T_c^{\omega\nu}x^{\omega\nu}$ as $x \rightarrow \infty$. The final term is an order $L^{-1/\nu}$ correction term. Although, with the parameters determined in [16] these 2 subleading terms are of similar size, it is easy to convince oneself that if the second term is omitted, a reasonable approximation to M over the range of interest can be obtained by readjusting parameters B and b_1 .]

Finite size scaling (with just the leading term of equation 14) apparently fails for the chiral condensates measured in our χ QCD simulations. It is therefore helpful to apply a finite size scaling analysis to the magnetization for $O(2)$ spin models, including the data from small lattices. To do this, we plot the scaling function $L^{\beta_m/\nu}M$ against the scaling variable $tL^{1/\nu}$. Close to the transition (t close to zero), for large enough lattices, the data for all lattice sizes should follow the same universal curve. Figure 10a shows this curve using $O(2)$ critical indices β_m and ν . Near $t = 0$ the curves for different lattice sizes coincide. As one moves away from $t = 0$ the curves start to diverge. As the lattice sizes increase the curves follow one another for larger ranges of $tL^{1/\nu}$, and it appears that they are approaching a universal curve. As can be seen, the small lattices do not follow the universal curve very far at all. While investigating such scaling, it is interesting to try other values for β_m and ν . Our earlier, but now suspect, identification of the $N_t = 6$ transitions as being tricritical, suggests we try the critical indices for a tricritical point, $\beta_m = 0.25$ and $\nu = 0.5$. The result is plotted in figure 10b. The initial impression is that this plot shows much better evidence for finite size scaling than that with the correct critical exponents. A closer look

reveals that it is the larger lattices that show significant departures from the ‘scaling curve’. This departure is small but significant for the 12^3 lattice, larger for the 16^3 lattice and embarrassingly large for the 24^3 lattice. However, it is clear that if we only had the smaller lattices, we would have concluded that the critical point was a tricritical point, not an $O(2)$ critical point. Unfortunately this is essentially the situation for the current round of lattice QCD simulations, so we need to be very careful.

VI. DISCUSSION AND CONCLUSIONS

We have simulated the finite temperature behaviour of lattice QCD with 2 flavours of staggered quarks using the χ QCD action which allows us to run at zero quark mass. Running with zero quark mass gives us direct access to the second-order phase transition from hadronic matter to a quark-gluon plasma, and allows us to study its universality class. Attempts at determining the nature of this transition for staggered quark actions from runs at finite mass had led to a state of confusion, since the scaling behaviour near the transition often appeared inconsistent with both the $O(4)$ universality class expected for the continuum theory and the $O(2)$ universality class which one would predict from considerations of the reduced symmetry of the staggered fermions. The fermion masses that one is forced to use with standard staggered actions are too large to clarify what is happening and some of the most ambitious simulations of staggered fermion lattice QCD thermodynamics do not even try to study the nature of the critical point. Notable exceptions include a recent study of this transition at infinite coupling which shows clear evidence for $O(2)$ universality [25], and a study of lattice QCD with 2 light adjoint quark flavours, where the chiral and deconfinement transitions are distinct [26], which also shows evidence for $O(2)$ universality of the chiral transition.

We present results for the finite temperature behaviour of 2-flavour lattice QCD with the χ QCD action on $12^3 \times 8$, $16^3 \times 8$ and $24^3 \times 8$ lattices. The decrease of the chiral condensate as the critical point was approached from below appeared to be too abrupt for $O(2)$ or $O(4)$ universality. However, we found that it was possible to fit the chiral condensates to the magnetization curves for an $O(2)$ spin model on relatively small lattices 5^3 – 9^3 . This indicates that the transition is consistent with $O(2)$ universality. The problems with more naive approaches to measuring the details of the critical behaviour of this transition is that

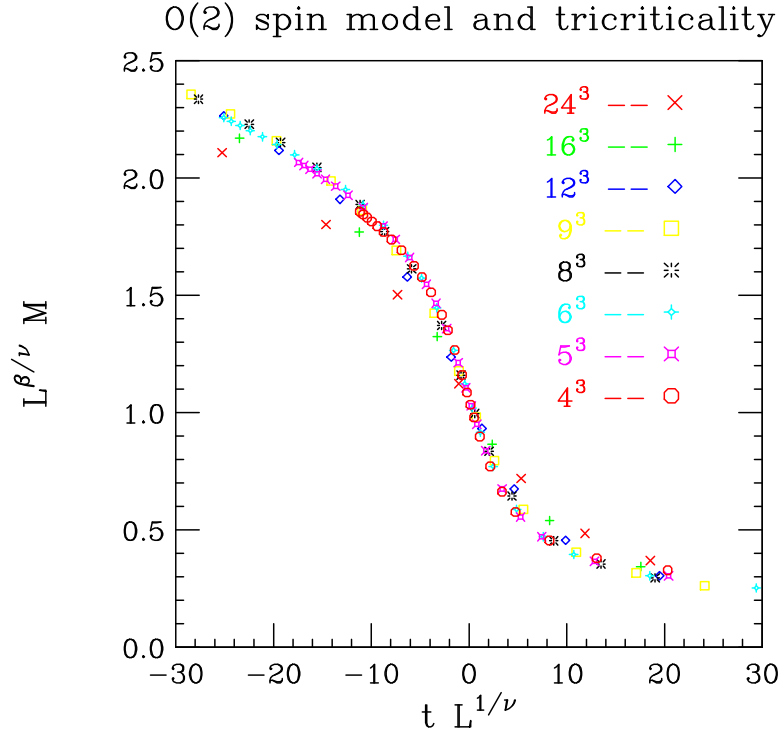
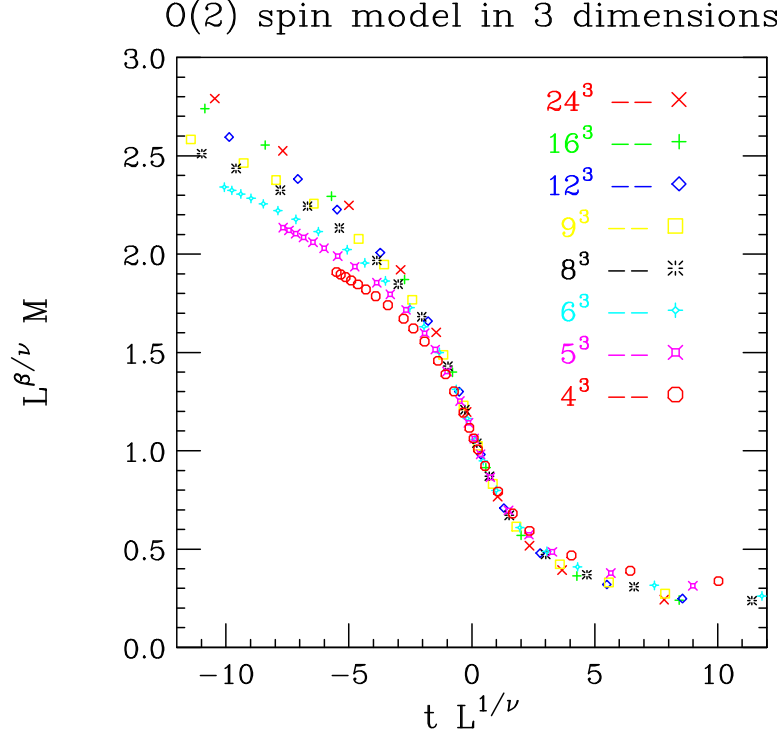


FIG. 10: a) Finite size scaling analysis for the magnetization for the $O(2)$ spin model. b) Same as (a) but using tricritical exponents instead of $O(2)$ critical exponents.

they do not adequately account for finite volume effects close to the transition, and that for

$O(2)$, the non-leading contributions to critical scaling are important except so close to the transition as to be inaccessible on the sizes of lattice we use. The spin model predictions for the correlation lengths and chiral susceptibilities for lattice QCD are similar enough to our measurements to add further support to this $O(2)$ interpretation. We also made fits to the condensates from our $18^3 \times 6$ simulations, which we had earlier interpreted as indicating tricritical behaviour, to the $O(2)$ spin model magnetizations on an 8^3 lattice. These fits were good enough to convince us that $N_t = 6$ simulations also yield results consistent with $O(2)$ universality.

A finite size scaling analysis of our $O(2)$ spin model magnetizations gave further clues as to why the behaviour of our lattice QCD measurements hinted at a tricritical explanation. The approach of the $O(2)$ spin model magnetizations to the universal finite size scaling curve with increasing lattice size is slow. However, if we perform a finite size scaling analysis using the critical exponents of the tricritical point, rather than those appropriate for $O(2)$, we find a rapid approach to an apparently universal curve with increasing lattice size. It is only by going to larger lattices, where the measurements start to diverge from this false scaling curve, that the tricritical interpretation is invalidated. For lattice QCD we do not at present have the luxury of being able to perform simulations on much larger lattices.

The results we presented in this paper are for a single small fixed value (in lattice units) of the 4-fermion coupling. It would be helpful if we could perform simulations at another (even smaller) value of this coupling, since the critical value of β , $5.535 \lesssim \beta_c \lesssim 5.536$ is significantly above that for the standard staggered action at $N_t = 8$, where reference [27] estimates $\beta_c = 5.44(3)$. We should also extend our analyses to finite quark masses to study critical scaling involving the critical exponent δ . We note that we could extend our current measurements to finite quark masses using Ferrenberg-Swendsen extrapolation. However, our attempts to do such an extrapolation indicated that this is only reliable for a range of masses where the condensate vanishes linearly with decreasing quark mass. For finite mass studies one needs quark masses large enough to get beyond this linear regime.

So far, we have only compared the critical behaviour of lattice QCD with the $O(2)$ spin model. We need to extend our studies to spin models in other universality classes as for example the $O(4)$ or the mean-field universality classes, before we can say with any certainty whether the evidence for $O(2)$ universality is compelling. Such studies are planned for the near future, since the spin-model simulations they involve are relatively inexpensive.

Finally, we need to address finite dt effects. We have found that finite dt effects can change the apparent nature of the phase transition in our studies of QCD at finite isospin chemical potential [28, 29] (see also [30]). There the problem was that the difference between the effective β , calculated by the equipartition theorem from the molecular-dynamics kinetic energies and the input β , a finite dt effect, was much larger below the transition than above, which distorted the transition. We have measured such β shifts in our χ QCD simulations, and while they are as large as those measured in our QCD at finite isospin simulations, they do not significantly change as we cross the transition, and are therefore unlikely to distort this transition. Nevertheless we intend to convert our simulations from hybrid molecular-dynamics to exact RHMC simulations [31]. Because the lower bound of the spectrum of the χ QCD Dirac operator is unknown, this is not an entirely trivial conversion. However, our experience with using the RHMC method to simulate QCD at finite isospin density, where the lower bound on the Dirac operator is also unknown, indicates that RHMC simulations *can* be applied in such cases [32].

Acknowledgements

These χ QCD simulations were performed on the IBM SP – Seaborg at NERSC, the IBM SP – Blue Horizon at SDSC/NPACI and the Tungsten cluster at NCSA. Access to the NSF machines was through an NRAC allocation. The spin model simulations we performed on linux PCs in the HEP Division of Argonne National Laboratory.

-
- [1] R. D. Pisarski and F. Wilczek, Phys. Rev. D **29**, 338 (1984).
 - [2] J. B. Kogut, J. F. Lagae and D. K. Sinclair, Phys. Rev. D **58**, 034504 (1998) [arXiv:hep-lat/9801019].
 - [3] C. W. Bernard *et al.*, Phys. Rev. D **54**, 4585 (1996) [arXiv:hep-lat/9605028].
 - [4] C. W. Bernard *et al.* [MILC Collaboration], Phys. Rev. D **56**, 5584 (1997) [arXiv:hep-lat/9703003].
 - [5] F. Karsch, Phys. Rev. D **49**, 3791 (1994) [arXiv:hep-lat/9309022].
 - [6] F. Karsch and E. Laermann, Phys. Rev. D **50**, 6954 (1994) [arXiv:hep-lat/9406008].
 - [7] S. Aoki *et al.* [JLQCD Collaboration], Phys. Rev. D **57**, 3910 (1998) [arXiv:hep-lat/9710048].

- [8] C. W. Bernard *et al.* [MILC Collaboration], Phys. Rev. D **55**, 6861 (1997) [arXiv:hep-lat/9612025].
- [9] C. W. Bernard *et al.*, Phys. Rev. D **61**, 054503 (2000) [arXiv:hep-lat/9908008].
- [10] G. Boyd, F. Karsch, E. Laermann and M. Oevers, arXiv:hep-lat/9607046.
- [11] E. Laermann, Nucl. Phys. Proc. Suppl. **63**, 114 (1998) [arXiv:hep-lat/9802030].
- [12] J. Engels, S. Holtmann, T. Mendes and T. Schulze, Phys. Lett. B **514**, 299 (2001) [arXiv:hep-lat/0105028].
- [13] J. B. Kogut and D. K. Sinclair, arXiv:hep-lat/0211008.
- [14] J. B. Kogut and D. K. Sinclair, Phys. Lett. B **492** (2000) 228.
- [15] J. B. Kogut and D. K. Sinclair, Phys. Rev. D **64**, 034508 (2001) [arXiv:hep-lat/0104011].
- [16] J. Engels, S. Holtmann, T. Mendes and T. Schulze, Phys. Lett. B **492**, 219 (2000) [arXiv:hep-lat/0006023].
- [17] A. Cucchieri, J. Engels, S. Holtmann, T. Mendes and T. Schulze, J. Phys. A **35**, 6517 (2002) [arXiv:cond-mat/0202017].
- [18] M. Hasenbusch and T. Török, J. Phys. A **32**, 6361 (1999) [arXiv:cond-mat/9904408].
- [19] H. G. Ballesteros, L. A. Fernandez, V. Martin-Mayor and A. Munoz Sudupe, Phys. Lett. B **387**, 125 (1996) [arXiv:cond-mat/9606203].
- [20] S. I. Tominaga and H. Yoneyama, Phys. Rev. B **51**, 8243 (1995) [arXiv:hep-lat/9408001].
- [21] F. Cooper, B. Freedman and D. Preston, Nucl. Phys. B **210**, 210 (1982).
- [22] M. N. Barber, in *Phase transitions and critical phenomena, Volume 8*, C. Domb and J. L. Lebowitz (editors), Academic Press, 145 (1983).
- [23] K. Binder, Z. Phys. B **43** (1981) 119.
- [24] A. M. Ferrenberg and R. H. Swendsen, Phys. Rev. Lett. **61**, 2635 (1988).
- [25] S. Chandrasekharan and F. J. Jiang, Phys. Rev. D **68**, 091501 (2003) [arXiv:hep-lat/0309025].
- [26] J. Engels, S. Holtmann and T. Schulze, Nucl. Phys. B **724**, 357 (2005) [arXiv:hep-lat/0505008].
- [27] S. A. Gottlieb *et al.*, Phys. Rev. D **55**, 6852 (1997) [arXiv:hep-lat/9612020].
- [28] J. B. Kogut and D. K. Sinclair, arXiv:hep-lat/0504003.
- [29] J. B. Kogut and D. K. Sinclair, arXiv:hep-lat/0509095.
- [30] O. Philipsen, PoS **LAT2005**, 016 (2005) [arXiv:hep-lat/0510077].
- [31] M. A. Clark and A. D. Kennedy, Nucl. Phys. Proc. Suppl. **129**, 850 (2004) [arXiv:hep-lat/0309084].

[32] J. B. Kogut and D. K. Sinclair (in preparation)